International Journal of Recent Technology and Engineering (IJRTE)
ISSN: 2277-3878 (Online), Volume-8 Issue-4, November 2019

Orthogonal Piezoelectric Energy Harvester for Low Frequency Applications: Modeling and Experimental Validation

N H H A Talib, H Salleh, M J Brennan

Abstract: ***The use of piezoelectric energy harvesters in low frequency applications is a classic problem due to the high elastic modulus of currently available piezoelectric materials. Furthermore, the output power is proportional to the third power of the excitation frequency. Higher excitation amplitudes or an increase in the piezoelectric material can produce a high output power. However, this is not feasible for weak environmental vibration, and using more piezoelectric material would incur a higher cost so this is not an attractive option. This article proposes an L-shaped piezoelectric energy harvester that amplifies the excitation amplitude with the aid of an extension arm. The effects of bending and rotational inertia are considered when modelling the open-circuit voltage that can be generated by the harvester. Experimental validation is carried out using zinc, aluminium and galvanized steel extension arms. The prediction model provides a good estimation of the results with acceptable error percentages for linear elastic extension arms. It is found that the proposed harvester geometry generates more output voltage for all lengths of extension arm, and the optimum lengths are different for each material. The use of a zinc extension arm generated 290 µW at 49 Hz, which is 55% greater than the power generated by a harvester without an extension arm that had a power density of 1.41 µW/mm^3.***

Keywords: ***Piezoelectric Energy Harvesters, High Output Power Zinc, Aluminium, Galvanized Steel.***

I. INTRODUCTION

In 1996, Williams and Yates [1] were the first to propose the possibility of generating electricity from mechanical vibrations using piezoelectric, electromagnetic and electrostatic mechanisms. Since then, vibration has been considered as a viable energy source and has been studied extensively. Beeby et al. [2] stated that the piezoelectric energy harvester offered the simplest approach compared to others and has received the most attention from researchers worldwide. The excellent performance of a piezoelectric energy harvester at high frequency is evident.

Manuscript published on November 30, 2019.
* Correspondence Author
N H H A Talib, Institute of Sustainable Energy, Universiti Tenaga Nasional, 43000 Selangor, Malaysia
H Salleh, Institute of Sustainable Energy, Universiti Tenaga Nasional, 43000 Selangor, Malaysia
M J Brennan, Department of Mechanical Engineering, São Paulo State University (UNESP), 01049-010 São Paulo, Brazil

However, vibration energy is most abundant at low frequencies, while commercial piezoelectric materials have a high Young's modulus [3], which means that they are more easily incorporated into devices targeting high frequency vibration. The low frequency vibration sources usually have low amplitudes, for example in human motions [4,5].

Furthermore, the output power of an energy harvester is proportional to the third power of the excitation frequency [6]. Therefore, the design of a low frequency piezoelectric energy harvesting device is challenging.

Dhakar et al. [7] proposed bonding a Lead Zirconate Titanate (PZT) bimorph onto a flexible Polyethylene Terephthalate (PET) beam to reduce the natural frequency. Their proposed harvester design was excited at 0.2 g and produced 40 µW of power at 36 Hz. This attempt improved the output power by 167% compared to the previous design involving a standalone bimorph, which only generated 15 µW at the much higher frequency of 125 Hz. Koven et al. [8] bonded a PZT plate beneath the base of a Polyurethane (PU) cantilever to separate the mechanical properties and natural frequency influences of the cantilever from the piezoelectric element. Using the d33 mode, their harvester generated 8.75 µW at 45 Hz when harmonically exited with an acceleration amplitude of 0.25 g. Ju and Ji [9] managed to harvest a higher output power of 269 µW at 20 Hz with an indirect impact-based energy harvester using a Macro Fiber Composite (MFC) beam. However, the extreme excitation of 3 g used in [9] is not realistic for many applications. Toyabur et al. [10] fabricated a multimodal energy harvester with four PZT beams. With an excitation level of 0.4 g, the peak output power reached 740 µW at 16 Hz. However, their proposed harvester suffered a 66% reduction of output power when only a single PZT beam was used.

High vibration amplitudes and more piezoelectric materials can compensate for the low output power when dealing with a low frequency source. These conditions are easily specified in laboratory; however, a different approach is needed for low frequency in a weak vibration environment. Such a typical application is a wireless sensor network (WSN), which can be potentially powered by the vibration energy of a train [11,12]. One of the reasons that WSN is used for intelligent automated monitoring systems is the affordable cost [13]. Thus, using more of the expensive piezoelectric materials to power the WSN would not be the best option. A more feasible way to overcome this limitation is to amplify the input vibration amplitude to the harvester, and this is the motivation for this paper.

The aim is to investigate the use of an extension arm to attach the piezoelectric energy harvester to the vibration source.

The extension arm amplifies the original vibration amplitude, resulting in an increase in the excitation at the base of the piezoelectric beam. This proposed device is called an orthogonal piezoelectric energy harvester (OPEH). It has a lower natural frequency and produces higher output power even with low excitation amplitudes when compared to a conventional design. The effects of the extension arm material and length on natural frequency and output voltage are investigated. The process starts with developing a model to represent the OPEH, which is then validated with experimental work.

II. HARVESTER DESIGN

This design proposed here employs a fixed-free boundary condition because it provides larger strain and lower natural frequency, which in turn results in higher output voltage compared to a beam with two fixed edges [14] or a simply supported beam [15]. The new design is shown in Fig. 1. It consists of a piezoelectric bimorph connected to the source of vibration orthogonally via a flexible extension arm to form an L-shape device. At the resonance frequency of the device, the extension arm amplifies the excitation amplitude of the piezoelectric bimorph. Furthermore, it reduces the natural frequency of the OPEH. The extension arm has seven 6 mm diameter holes, approximately 10 mm apart. The holes were used as points to clamp the device to the vibrating source, and to adjust the extension arm length during the experiment. Several commonly available materials were used for the extension arm, i.e., zinc, aluminium and galvanized steel. Each extension arm had a different thickness depending on the availability of each material.

The piezoelectric bimorph was bolted to the extension arm through a customized PTFE clamp. To further reduce the overall natural frequency of the structure four layers of Neodymium mass (NdFeb) were attached at the free end of the piezoelectric bimorph.

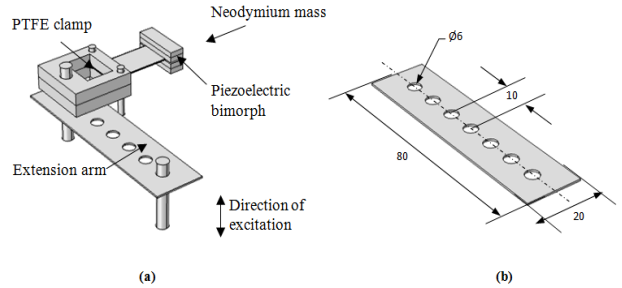

Fig. 1 (a) Schematic diagram of the orthogonal piezoelectric energy harvester (OPEH) and (b) details of the extension arm. All dimensions are in mm

III. ANALYTICAL MODELING

A simplified lumped parameter model (LPM) is developed to capture the dynamic behavior of the device e.g., displacements at the free end of the extension arm and piezoelectric bimorph. The modelling method is based on a study performed by Erturk and Inman [16]. They showed that a LPM provided a good estimation of the fundamental natural frequency and introduced a correction factor for the LPM to predict the motion at the tip when excited at its first natural frequency. The study revealed that as the ratio of tip mass to beam mass increased, the correction factor approached unity. Thus, this approach can be used if the tip mass is significantly larger than the beam mass, which is the case in the design proposed in this paper.

Deflection Due to Bending

Assuming free vibration, the deflection of the extension arm and piezoelectric bimorph due to bending can be determined by modelling the OPEH as the two degree of freedom (2DOF) system shown in Fig. 2.

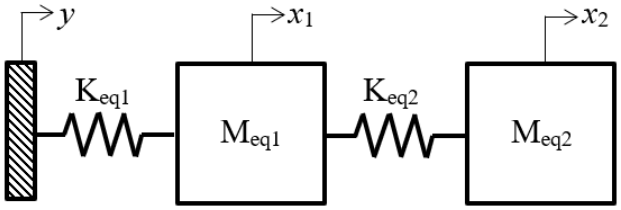

Fig. 2 2DOF Model of the OPEH under harmonic base excitation

The governing damped equations of motion for the system in Fig. 2 are given by

$$M_{eq1}\ddot{x_1} + K_{eq1}(x_1 - y) - K_{eq2}(x_2 - x_1) = 0 \quad (1)$$

$$M_{eq2}\ddot{x_2} + K_{eq2}(x_2 - x_1) = 0 \quad (2)$$

Where $M_{eq}$and K_{eq} are the equivalent massand stiffness, respectively, in which

$$M_{eq\ 1,2} = \frac{33}{140}m_{1,2} + m_{3,4} \quad (3)$$

$$K_{eq\ 1,2} = \frac{3E_{1,2}I_{A\ 1,2}}{{L_{1,2}}^3} \quad (4)$$

Where the subscripts 1, 2, 3 and 4 relate to the extension arm, piezoelectric beam, PTFE clamp and tip mass respectively. The equivalent mass is the summation of partial cantilever beam mass,$m_{1,2}$ and tip mass, $m_{3,4}$[17]and calculated based on equation 3.The equivalent stiffness is determined by using equation 4 where$E$ is the Young's modulus, I_A is the area moment of inertia and L is the effective length.x is the beam deflection and y is the base displacement.Since the piezoelectric bimorph is reinforced with brass, a general rule of mixtures is used to predict the corresponding Young's modulus. For a rectangular beam cross section, the moment of inertia is given by $I_{A\ 1,2} = \frac{W_{1,2}{T_{1,2}}^3}{12}$where W and T are the effective width and thickness, respectively. Suppose the base is harmonically excited (common practice in energy harvesting literature), the natural frequencies, ω_n of first and second vibration modes are determined by solving

$$\begin{vmatrix} K_{eq1} + K_{eq2} - {\omega_n}^2 M_{eq1} & K_{eq2} \\ -K_{eq2} & K_{eq2} - {\omega_n}^2 M_{eq2} \end{vmatrix} = 0 \quad (5)$$

The vibration responses $x_1(t)$ and $x_2(t)$ are obtained via modal analysis [18]. The solutions are given by

$$x_1(t) = q_{11}q_{11}K_{eq1}Y\omega\left[\frac{1}{\omega_1^2-\omega^2}\right]\left[\frac{1}{\omega}sin\,\omega t - 1\omega 1sin\omega 1t + q12q12Keq1Y\omega 1\omega 2\,2-\omega 21\omega sin\omega t - 1\omega 2sin\omega 2t\right] \quad (6)$$

Where q_{11}, q_{12}, q_{21} and q_{21} are determined from the mass-normalized matrix of eigenvectors, Y is the amplitude of base displacement and ω is the excitation frequency. The relative displacement $x_B = x_1(t) - x_2(t)$ is related to the mechanical stress of the piezoelectric beam, which in turn is related to the electrical energy generated by the device.

Deflection Due to Rotational Inertia

Continuous base excitation causes the piezoelectric beam to carry a significant momentum and produce an effect of rotational inertia. The piezoelectric beam exerts a torsional moment to the extension arm, causing an angular deflection. To identify this deflection magnitude, the OPEH is modelled as a single cantilever beam subjected to torsional vibration as shown in Fig. 3.

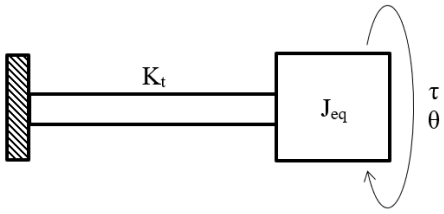

Fig. 3 Torsional vibration of a cantilever beam

The governing equation of motion is given by

$$J_{eq}\ddot{\theta} + K_t\theta = \tau \quad (8)$$

Where $J_{eq} = \frac{Meq_1}{12}(T_3{}^2 + W_3{}^2)$is the equivalent polar moment of inertia, where T and W are the thickness and width, respectively.$K_t = \frac{JG_1}{L_1{}_t}$ is the torsional stiffness, where $J \approx W_1T_1{}^3\left[\frac{1}{3} - 0.21\frac{T_1}{W_1}\left(1 - \frac{T_1{}^4}{12W_1{}^4}\right)\right]$ is torsional constant for a rectangle, and G is the shear modulus. The torque transmitted by the OPEH, τ is related to its angular acceleration,α by

$$\tau = I_M\alpha \quad (9)$$

Where $I_M = \frac{m_2}{3}L_2^2 + \frac{m_4}{12}\left(\frac{L_4^2}{2}\right) + m_4\left(L_2 + \frac{L_4}{2}\right)^2$ is the OPEH's mass moment of inertia attained by superposition of the moments of its components parts, and $= \frac{\omega_d{}^2x_1(t)}{L_2}$. The additional deflection of piezoelectric beam contributed by rotational inertia effect is given by

$$x_R = W_1\sin\theta \quad (10)$$

where $\theta = \frac{\tau}{K_t - J_{eq}\omega_d{}^2}$is the angular deflection of extension arm.

Output Voltage and Power

The open circuit voltage [19] generated by the OPEH operating in 31-mode is determined by substituting the deflection magnitudes due to bending and rotational inertia effects into equation

$$V_{OC} = \frac{3T_2{}^2d_{31}E(x_B+x_R)}{2L_2{}^2\varepsilon_{33}^T} \quad (11)$$

Where d_{31} is the piezoelectric strain coefficient, ε_{33}^T is the permittivity and $E$is the Young's modulus of the PZT bimorph beam.

The output power can be estimated by considering the The venin equivalent circuit shown in Fig. 4. The internal impedance of the PZT bimorph, Z_I is a capacitive type [20]. Thus, the effective internal impedance is equal to the capacitive reactance, X_C given by

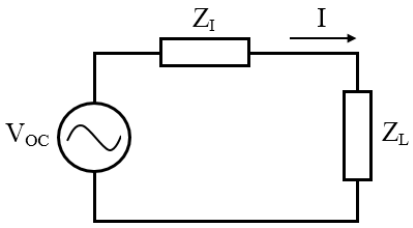

Fig. 4 Equivalent electric circuit of OPEH

$$Z_I = X_C = \frac{1}{\omega_n C} \quad (12)$$

Where C is the capacitance value of series-connected PZT bimorph. The maximum power can be transferred when the load impedance, Z_L matches the internal impedance i.e. $Z_L = Z_I = X_c$. The output power, P_L is the given by

$$P_L = \frac{V_{OC}{}^2}{4Z_L} \quad (13)$$

IV. EXPERIMENTAL PROCEDURE

An energy harvester without an extension arm, and the OPEH experimental setup are shown in Fig. 5. The parameter values of the piezoelectric material, magnets and all four types of extension arm are provided in Table 1. A PZT bimorph (PSI-5H4E) with overall dimensions of 31.8 mm×12.7 mm×0.51 mm was used in the construction of both devices. The top and bottom surfaces were primed with the special flux, prior to soldering the tinned copper wire (26 AWG). For the OPEH, the PZT beam was then clamped and attached to the extension arm (two sizes of cap screw used i.e. M5×30, M5×20), which was then fixed to the shaker by using another cap screw of size M5×25. The shaker was supplied by the excitation signal from a harmonic function generator passed through a power amplifier and acted as a vibration source for the energy harvester. The system was excited in the frequency range 15-105 Hz with a constant input acceleration of 0.25±0.02 g_{rms}, which was monitored using an accelerometer. Vibration data was acquired using a National Instrument four channel dynamic acquisition system. The open circuit voltage at each frequency was measured by using a multimeter. The procedure was repeated for OPEH with all extension arm material and length. The frequencies at which the harvester produced peak voltages were noted and assumed to be their natural frequencies. Both frequency and open circuit voltage data were used to validate the analytical model suggested.

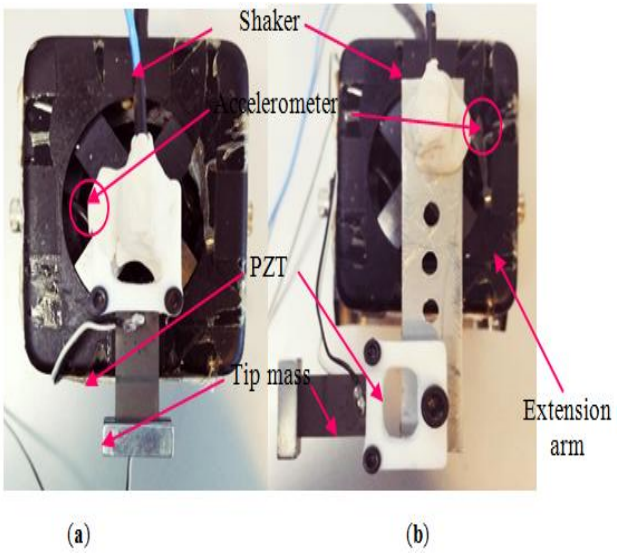

Fig. 5 The test setup of (a) control harvester, and (b) OPEH with zinc extension arm

Table. 1 Parameters of piezoelectric element and beam structure

Material	Parameter	Value	Unit
PZT (PSI-5H4E)	T	0.382	mm
	E	62	GPa
	ρ	7800	kg/m^3
	Q	32	-
	d_{31}	-320×10^{-12}	m/V
	ε_{33}^{T}	3.009×10^{-8}	F/m
	k_{31}	0.44	-
	C_{series}	24	nF
Brass	T	0.128	mm
	E	125	GPa
Magnet (NdFeB)	L	5	mm
	m_t	6.96×10^{-3}	kg
Zinc	T	0.6	mm
	E	110	GPa
	ρ	5913.3	kg/m^3
	ζ	0.01	-
Aluminium	T	1.1	mm
	E	69	GPa
	ρ	2658.4	kg/m^3
	ζ	0.01	-
Galvanized steel	T	1.4	mm
	E	220	GPa
	ρ	7664	kg/m^3
	ζ	0.01	-

Next, the output powers of control harvester and selected OPEH (natural frequency ≈ 50Hz) were determined by connecting them to a resistor. In this experiment, a potentiometer (B1M) was connected to the circuit as a variable resistor and the testing range was determined based on the estimated value. The output power was calculated directly after each measurement of voltage across the resistor, V_L to identify its peak by using $P_L = \frac{{V_L}^2}{Z_L}$.

V. RESULTS

Starting with the experimental result of control energy harvester, a peak voltage of 8.13 V_{rms} was generated at 75 Hz. Then, the accuracy of the predicted natural frequency of OPEH was investigated. Figure 6 presents the results of first natural frequency obtained from the model and experiment. As anticipated, the natural frequency of energy harvester reduced when the extension arm was introduced. There is a clear trend of decreasing natural frequency as the extension arm becomes longer. It is also apparent that the first predicted and experimental natural frequencies closely match. The highest variation percentage of 11.32% was recorded for OPEH with zinc extension arm (L_1=40mm). The model was reliable to predict the first natural frequency. Figure 6 also shows that the OPEH with galvanized steel extension arm had (L_1=30mm) the highest natural frequency of 66Hz, certainly due to its thickness and largest Young's modulus, while the lowest frequency of 19Hz was recorded by the one with zinc extension arm (L_1=70mm).

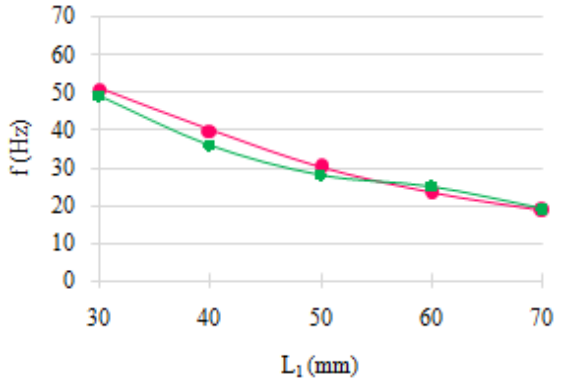

(a)

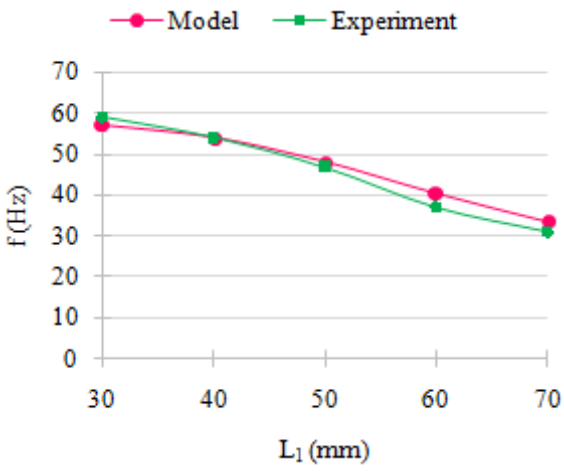

(b)

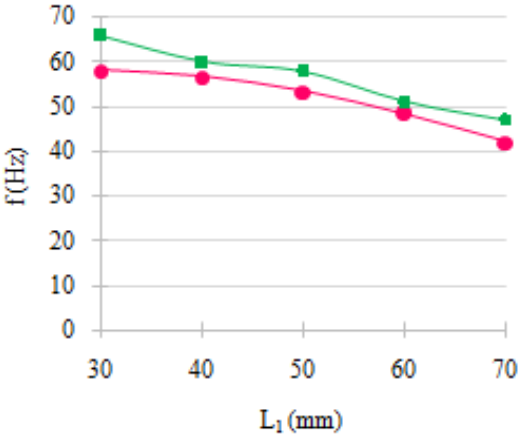

(c)

Fig. 6 First natural frequencies at corresponding (a) zinc, (b) aluminium, and (c) galvanized steel extension arm's lengths

Turning now to the experimental evidence of the model validity to estimate the open circuit voltage. It was found that the peak voltage was much more significant at the first natural frequency than the second one for all setup. Figure 7 compares the predicted output voltage with those obtained experimentally at corresponding first natural frequency. The variation percentages were 17% at most. What stands out in the figure is that the trend of output voltage was different from each other. It is rather interesting that there were different ideal extension arm's lengths for different materials. The highest output voltage of 14.23V_{rms} was generated by OPEH with zinc extension arm (L_1=60mm) at 25Hz. The OPEH with galvanized steel extension arm (L_1=70mm) produced the lowest output voltage of 8.67V_{rms} which is still larger than the output voltage of control harvester.

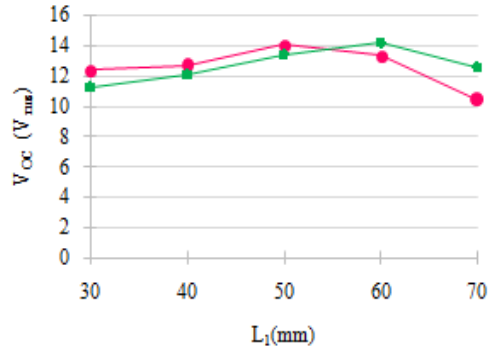

(a)

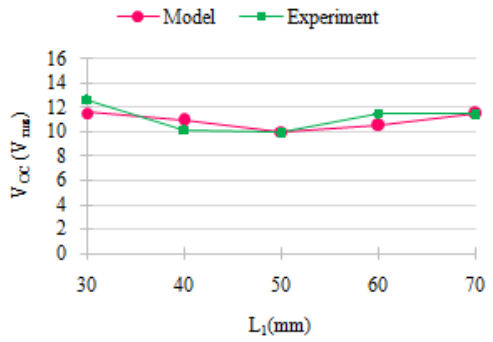

(b)

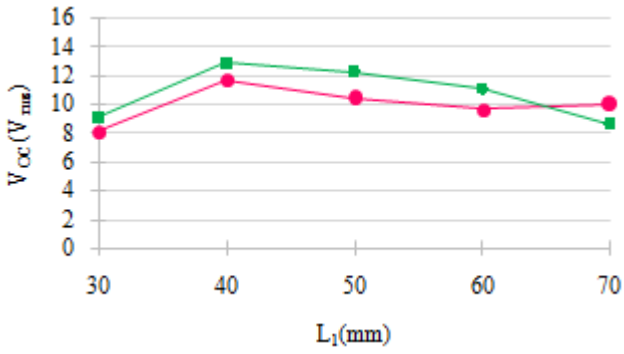

(c)

Fig. 7 Resonance open circuit voltages at corresponding (a) zinc, (b) aluminium, and (c) galvanized steel extension arm's lengths

The experiment was further conducted to identify the optimum load resistance and AC output power of control energy harvester and OPEH that had a natural frequency around 50Hz i.e. with zinc (L_1=30mm) and aluminium (L_1=50mm). The predicted and experimental results are tabulated in Table 2. Equation 12 provides good estimation of optimum load resistance of the three tested harvesters with variations of 8.09%, 6.67% and 1.68%, respectively. The control harvester supplied 48.09% of voltage to the load while OPEH with zinc and aluminium extension arms transferred 52.57% and 56.74%, respectively. In terms of output power, the difference between the calculated value from equation 13 and experimental result is most significant for OPEH with aluminium extension arm. Previous works [21,22] reported model validation results with more or less 20% variation. Thus, it can be deduced that the prediction method contributes reliable estimation of the experimental results.

Table. 2 Comparison of load resistance and AC output power of control harvester and OPEH

	Parameters	Prediction	Experiment	Unit	Variation
Control	f		75	Hz	
	$Z_I = Z_L$	88	82	kΩ	8.09%
	V_{OC}	8.3	8.1	V_{rms}	2.21%
	V_L	4.2	3.9	V_{rms}	6.39%
	P_{AC}	195	187	µW	4.63%

OPEH with Zinc (L_1=30mm)	f	51	49	Hz	4.08%
	$Z_I = Z_L$	130	122	kΩ	6.67%
	V_{OC}	12.4	11.3	V_{rms}	9.65%
	V_L	6.2	5.9	V_{rms}	4.38%
	P_{AC}	296	290	µW	1.97%
OPEH with Aluminium (L_1=50mm)	f	48	47	Hz	2.13%
	$Z_I = Z_L$	135	133	kΩ	1.68%
	V_{OC}	10.2	9.9	V_{rms}	3.02%
	V_L	5.1	5.6	V_{rms}	9.22%
	P_{AC}	194	239	µW	18.95%

VI. DISCUSSION

The present work was designed to propose the OPEH and determine the effects of extension arm's material and length on natural frequency and output voltage. It was hypothesized that OPEH reduced the natural frequency and produced higher output power at low excitation amplitude. This section is set out to firstly discuss on the natural frequency of OPEH. All recorded values were indeed less than that of the control energy harvester with the expected decreasing trend as the arms became longer. OPEH with zinc extension arm had the lowest natural frequency range despite its higher Young's modulus when compared to aluminium, certainly due to its thinner body. A notable fact of 2DOF system is that there are two vibration modes corresponding to two natural frequencies. Surprisingly, the prediction model did not provide a good estimation of the second natural frequency in which the predicted values were significantly larger than the experimental results. In general, damping reduces the amplitude of resonance peak and causes the peak to occur at lower frequency. Hence, a possible explanation to this might be that the second vibration mode is more affected by the damping than the first natural frequency. Unlike the SDOF system in which its damped natural frequency always tends to be lower than the undamped frequency, Caughey and O'Kelly [23] explained that multi-DOF system with classical normal modes always has the damped natural frequency less or equal to the corresponding undamped frequencies. It was also reported that the highest natural frequency is always reduced by damping.

Secondly, the results also indicate that OPEH produced at least 1.62 times the open circuit voltage of the control energy harvester for all extension arms' conditions. One important finding is the phenomenon of optimum length that is consistent with the findings of Egg born [24] and Mine to et al.[25]. When a certain beam length is reached, the overall characteristics of the system start to change, modifying the effective cross section, Young's modulus and natural frequency. This adversely affects the beam deflection and strain experienced by the piezoelectric bimorph, hence the output voltage and power produced.

The section is finally dedicated to assessing the capability of OPEH to generate higher output power at lower frequency. Based on the equation 12, it is anticipated that lower natural frequency results in higher optimum load resistance which undesirably reduces the current flow as well as the voltage across the resistor (Ohm's law). Nevertheless, the OPEH with zinc (L_1=30mm) and aluminium (L_1=50mm) extension arms generated 55.36% and 28.07% more output power than the control harvester at two-third of its natural frequency. The comparison could be more meaningful if the control harvester is adjusted to work at the same frequency. However, reducing the natural frequency of control harvester to 50Hz required more tip mass (as the cantilever dimension should be fixed) that the bimorph beam snapped upon excitation. The largest power density obtained in this work is 1.41µW/mm^3.

VII. CONCLUSION

This work set out to propose an orthogonal piezoelectric energy harvester for low frequency weak vibration applications. The effect of bending and rotational inertia had been incorporated into the prediction model. Whilst the model did not predict the second natural frequency, the experiment confirmed that the model provides good estimation of the fundamental natural frequency, and corresponding open circuit voltage and output power. The first major finding is that, compared to the control energy harvester, the OPEH generated more open circuit voltage for all extension arm's lengths. The second major finding is the unique trend of output voltage for each extension arm in which the maximum value was produced with different optimum length. Taken together, these findings suggested a role for extension arm in boosting the output power of the orthogonally connected energy harvester especially in low frequency weak vibration environment.

The present work appears to be one of the first attempts to exploit the torsional moment for larger piezoelectric bimorph deflection which has been explicitly demonstrated. However, being limited to linear elastic material, this work lacks a proper model for nonlinear elastic extension arm. Therefore, it is recommended that future work involves modelling for OPEH with nonlinear elastic extension arm. Furthermore, it would also be interesting to identify the real output power considering the diode voltage drop in energy harvesting circuit. Then, the harvester could also be tested in real random ambient vibration. Following model validation, this ongoing work will proceed with application of other parameters as well as optimization of the output power at 50Hz. The output power might be boosted by coating the piezoelectric bimorph with rubber compound as proven by Resali et al. [26].

ACKNOWLEDGMENTS

This work was supported by Ministry of Higher Education Malaysia, Fundamental Research Grant Scheme grant number 20140133FRGS and the Uniten Internal Grant J510050869

REFERENCES

1. C. B. Williams's and. B. Yates, Sensor Actuat APhys52, 8–11 (1996).
2. S.P Beeby, M. J. Tudor and N. M. White, Meas Sci Technol, 17 (2006).
3. H. Li, C. Tian andZ. D. Deng, ApplPhys Rev 1, 041301 (2014).
4. M. Z. Nuawi, A. R. Ismail, M. J. M. Nor and M. M. Rahman, International Journal of Automotive and Mechanical Engineering4, 490-503 (2011).
5. A.R Ismail, S. N. A. Abdullah, A. A. Abdullah and B. M. Deros, International Journal of Automotive and Mechanical Engineering11, 2786-2792 (2015).
6. T. M.Kamel, R.Elfrink, M. Renaud, D. Hohlfeld, M. Goedbloed, C. D. Nooijer, M. Jambunathan and R. V. Schaijk, JMicromech Microeng 20, 105023 (2010).
7. L.Dhakar, H. Liu, F. Tay and C. Lee, Sensor ActuatAPhys199, 344–352 (2013).
8. R. Koven, M. Mills, R. Gale and B. Aksak, IEEE Trans Ultrason Ferroelectr Freq Control 64, 1735–1743 (2017).
9. S. Ju and C. H. Ji, 18th International Conference on Solid-State Sensors, Actuators and Microsystems, (2015).
10. R. M. Toyabur, M. Salauddin and J. Y. Park, CeramInt43, S675-S681 (2017).
11. V. G. Cleante, M. J. Brennan, G. Gatti and D. J. Thompson, Journal of Physics: Conference Series 744,012080 (2016).
12. G. Gatti, M. J. Brennan, M. G. Tehrani and D. J. Thompson, Mech Sys Signal Process66-67, 785-792 (2016).
13. Y. Han, Y. Feng, Z. Yu, W. Lou and H. Liu, IEEE Sens J17, 6770-6777 (2017).
14. A. S. Kherbeet, H. Salleh, B. H. Salman and M. Salim, Sustainable Energy Technologies and Assessments11, 42-52 (2015).
15. Z. Li, G. Zhou, Z. Zhu and W. Li, Energies9,98 (2016).
16. A. Erturk and D. J. Inman, J Intell Mater Syst Struct19,1311-1325 (2008).
17. S. S. Rao, "Mechanical Vibrations"(New Jersey: Prentice Hall, 2011)
18. Information onhttps://vibrationdata.wordpress.com
19. A. Nechibvute, A. R. Akande and P. V. Luhanga, Pertanika J Sci Technol19, 259-271 (2011).
20. W. G. Ali and S. W. Ibrahim, Energy and Power Engineering 4, 496-505 (2012).
21. H. Y. Wang, X. B. Shan and T. Xie, J Zhejiang Univ-Sci A (Appl Phys &Eng) 13, 525-537 (2012).
22. L. G. H. Staaf, E. Koehler, D. Parthasarathy, P. Lundgren, P. Enoksson, Sensor Actuat APhys 229, 136-140 (2015).
23. T. K. Caughey and M. E. O'Kelly, JAcoustSoc Am33, 1458-1461 (1961).
24. T. Eggborn, "Analytical models to predict power harvesting with piezoelectric materials" (Virginia Polytechnic Institute and State University, 2003).
25. A. T. Mineto, M. Pereira, D. S. Braun and E. Harvesting, DINCON 2010: 9th Brazilian Conference on Dynamics, Control and Their Applications, (2010).
26. M. S. M. Razali and H. Salleh, JMech Eng 2, 199-214 (2017).
27. Manikanthan, S.V., Padmapriya, T., "An efficient cluster head selection and routing in mobile WSN" International Journal of Interactive Mobile Technologies, 2019.
28. Hussain, A., Manikanthan, S.V., Padmapriya, T., Nagalingam, M., "Genetic algorithm based adaptive offloading for improving IoT device communication efficiency", Wireless Networks, 2019.